Int J Adv Struct Eng (2015) 7:261–267
DOI 10.1007/s40091-015-0097-2

ORIGINAL RESEARCH

Behavior of reinforcement SCC beams under elevated temperatures

Hamoon Fathi[1] · Kianoosh Farhang[1]

Received: 11 September 2014 / Accepted: 4 July 2015 / Published online: 18 July 2015

Abstract This experimental study focuses on the behavior of heated reinforced concrete beams. Four types of concrete mixtures were used for the tested self-compacting concrete beams. A total of 72 reinforced concrete beams and 72 standard cylindrical specimens were tested. The compressive strength under uniaxial loading at 23 °C ranged from 30 to 45 MPa. The specimens were exposed to different temperatures. The test parameters of interest were the compressive strength and the temperature of the specimens. The effect of changes in the parameters was examined so as to control the behavior of the tested concrete and that of the reinforced concrete beam. The results indicated that flexibility and compressive strength of the reinforced concrete beams decreased at higher temperatures. Furthermore, heating beyond 400 °C produced greater variations in the structural behavior of the materials in both the cylindrical samples and the reinforced concrete beams.

Keywords Self-contacting concrete · Elevated temperature · Reinforcement beam · Cracks patterns

Introduction

Designing fire-resistant concrete structures requires further laboratory studies for examining the behavior of concrete and concrete structures (i.e., beams, columns, and joints) under extreme temperatures. Mechanical behavior modeling of concrete at different temperatures plays an important role in the structural analysis of concrete when it is exposed to fire. Being a combination of concrete and steel, concrete structures tend to show an even more complex behavior under high temperatures.

The physical and mechanical properties of concrete and concrete beams alter with increasing temperature. Being exposed to fire and high temperatures would increase the compressive strength and modulus of elasticity of concrete (Cioni et al. 2001; Sancak et al. 2008; Huang and Burgess 2012; Mydin and Wang 2012). Numerous studies have been conducted on tensile strength and the stress–strain relationship in concrete specimens. Due to differences in the applied materials as well as specimen size, experimental parameters, and test conditions, it is not easy to compare the obtained results under different fire conditions (Carreira and Chu 1985; Youssef and Moftah 2006; Chang et al. 2006). Models of stress–strain, modulus of elasticity, and compressive strength at high temperatures are required for analysis of concrete structures under fire attack. Numerous researchers have endeavored to simulate the behavior of concrete at high temperatures (Khennane and Baker 1993; Terro 1998; Ranzi and Bradford 2007; Huang et al. 2009), by proposing models for predicting the behavior of concrete at high temperatures using different concrete mixtures. Aggregates and additives type as well as specimens size can affect the proposed models. Because of such variations, it is impossible to draw a comparison between the proposed models and experimental outcomes.

High construction costs and laboratory conditions make examinations of full-scale concrete and steel structures difficult. For this reason, most large-scale structures are modeled through computer software. In certain cases, structural components (beams and columns) are tested using computer programs to provide behavioral models.

✉ Hamoon Fathi
fathi.hamoon@gmail.com

[1] Department of Civil Engineering, Sanandaj Branch, Islamic Azad University, Sanandaj, Iran

The studies on behavior of structural components mainly concentrate on beams, columns, and joints (connections). A laboratory study deals with short reinforced concrete columns exposed to heating and cooling processes (Huo et al. 2013). In their studies, researchers have examined the effects of a uniaxial load on columns during the fire (Xu and Wu 2009), demonstrating that the strength of heated concrete columns at different cross sections was related with the axial force exerted on the columns. Ultimately, the behavior of concrete was modeled through numerical simulations at different thermal strengths.

Tan and Nguyen (2013) examined the uniaxial flexural effects on heated reinforced concrete columns. They tested six specimens with an average height of 3.3 m and square cross section of 300 mm, and found that a significant relationship existed between the specimen dimensions and the behavior thereof under temperature. In other studies, the behavior of concrete and reinforced concrete beams (RCBs) was studied under temperature rise at various fire intensities (Tan and Zhou 2011; Kim et al. 2012). Moreover, Dwaikat and Kodur (2009) tested several RCBs with different compressive strengths under fire conditions, examining the impact of fire on concrete beams with high compressive strength. High compressive strength in concrete leads to extreme variations when comparing temperature effects on the behavior of concrete beams.

Nowadays, there is an increasing demand for application of self-compacting concrete (SCC). Plasticizers and additives with various properties are also applied in preparation of SCC so as to influence the thermal behavior of concrete. Equally important is the impact of such materials on the behavior of concrete beams as a combination of steel and concrete. This study aims to evaluate the effect of temperature on the SCC applied in experiments with various strengths as well as to examine the effect of temperature on the compressive strength variations in concrete. In a different section of the study, concrete beams are constructed with the same concrete mixture and placed under post-heating flexural loading. Finally, a model is proposed to predict the moment–curvature behavior of RCBs.

Materials and methods

In this study, the effect of temperature on SCC and RCB flexural was examined through experiments involving several cylindrical specimens and concrete beams based on the specifications and materials introduced in this section.

The mixtures

The concrete mix used in the experiments consists of crushed gravel, micro silica, plasticizer, cement, and water. They were prepared from local sources (Table 1).

Seventy-two (section diameter: 150 mm, high: 300 mm) standard cylindrical specimens and seventy-two reinforcement concrete beams were tested. The compressive strength of the specimens manufactured with respect to the different mix plans at 23 °C is 30, 35, 40, and 45 MPa (Table 2). Specifications of the manufactured concrete mixes are categorized in four different groups (SCC1–SCC4). The amount of micro silica is changed and other proportions of materials were constant. The results of liquefaction experiments on the behavior of SCC specimens are given in Table 2.

Specimens

The constructed concrete specimens were of two types: RCBs (250 mm × 250 mm × 1000 mm) and standard

Table 1 Specifications of materials

Materials name	Materials type	Qualification
Aggregate	Gravel	Bulk: 1750 kg/m^3; maximum size: 19.5 mm
Water	Normal	pH: 7; low mineral
Cement	Type 1	Setting time: 135 min, compressive strength: 325 kg/cm^2
Add materials	Micro silica	Density: 2110 kg/m^3
	Plasticizer	Density: 1200 kg/m^3

Table 2 Self-compacting concretes mixes

Name	Cement weight ratio (375 kg in 1 m^3)			Slump flow (diameter) cm	Compressive strength (cylinder) MPa
	$\frac{\text{Plasticizer}}{\text{Cement}}$ (%)	$\frac{\text{Microsilica}}{\text{Cement}}$ (%)	$\frac{\text{Water}}{\text{Cement}}$ (%)		
SCC 1	4	0	30	68	30
SCC 2	4	4	30	66	35
SCC 3	4	8	30	62	40
SCC 4	4	12	30	60	45

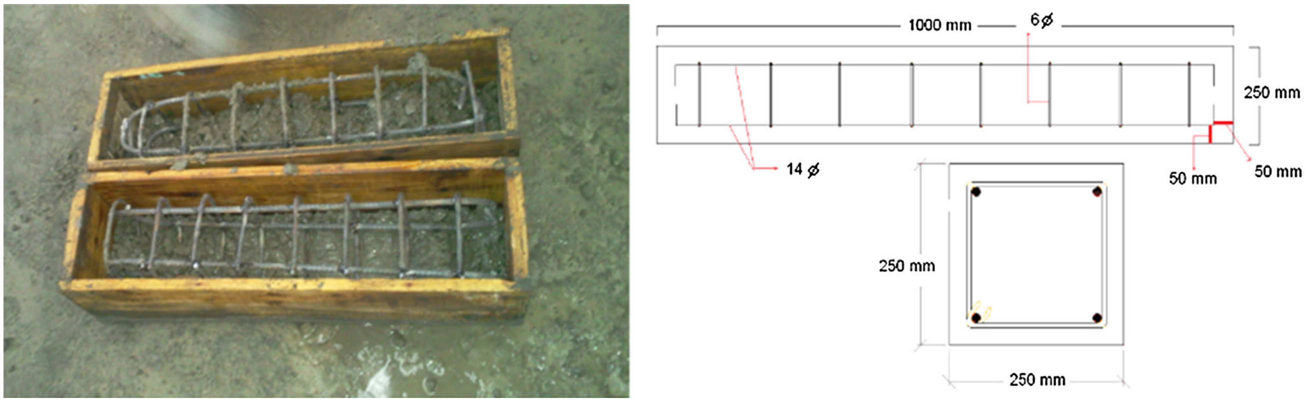

Fig. 1 Mesh reinforcement concrete beam and specimens

cylinders (150 mm × 300 mm). Seventy-two, one meter RCB specimens and seventy-two standard cylinders were tested. The reinforcing mesh in RCB included four rebars with a 14 mm in diameter and a total of 8 stirrups with a diameter of 60 mm (Fig. 1). The reinforcing mesh was embedded within an external 50 mm coating. Several concrete spacers were applied to properly control the effects of the applied heat. The concrete applied in construction of beams and cylindrical specimens was made of SCC with four different compressive strengths introduced in Table 2. The rebars applied in the RCBs were made of E60 steel.

Curing

For preparing and standardizing materials, stone seeds were washed, dried, and drowned in water for 24 h with room's temperature (23 °C). Stone seed surfaces are dried to accomplish standard surface dry (SSD) mood. The required water for concrete was added in two stages before and after adding additive and plasticizer. After 24 h, frames were removed and samples were placed in mixture of water and some lime for 27 days. Lime was used for reducing alkaline condition. The amount of lime added to the specimen-holding pool was about 1.5 kg/m^3. The 28-day cured RCB was heated in oven and the next day after cooling the beam, it was loaded with quasi-static rate. Compressive strength and temperature were the variable parameters in this experimental part. The beneath of the beam was heated for simulating natural behavior of fire accidents and compressive force is exerted from upper side and from the center of the beams. They were subjected to heating, loading, and testing. Actually, the air holes in the specimens were not dry but the effects of that water is negligible (Lo et al. 2009). The specimens were allowed to cool naturally to room temperature.

Test machine

The constructed specimens had four different compressive strengths, and were heated and tested at six different temperatures (23, 100, 200, 400, 600, and 800 °C). The heating rate was 10 °C/min. The cylindrical specimens were tested under uniform compressive uniaxial loading. The concrete beams were placed under uniaxial loading at the center and the flexure applied to the beams was controlled. A loading rate of about 5 KN/s was deployed within the quasi-static range. The loading span of the concrete beam between two abutments 900 mm apart was in the form of point loading. The axial deformation of cylinders and the center of the concrete beam were controlled (Fig. 2). The deformation diagram was drawn based on the obtained strain. This diagram illustrates the deformations caused by the exerted stress and heat prior to loading.

Results and discussion

In this section, the impact of heat on the compressive and flexural strengths and mechanical properties of concrete were studied and compared. The concrete beams were heated on one side so as to create a real-world model of a beam buried in the concrete ceiling. In fact, the concrete beam was coated with fiberglass and ceramic-covered walls in five different directions, and the furnace heat affected the beam in one direction.

The effect of heat on flexural and compressive strength of concrete

From each composition of concrete mixture (specified by SCC1–SCC4), three cylindrical specimens and three RCB specimens were heated to different temperatures. The results for these specimens were obtained through

Fig. 2 Test machine (**a** heater, **b** bending test, **c** compressive test, **d** V funnel test, **e**, **f** slump flow test)

interpolation and introduced as the mean strength and deformation values.

Studies have shown that rising temperatures reduce the flexural strength of RCBs (Fig. 3). Furthermore, the rate of variations in the diminishing flexural strength is accompanied by certain variations both below and above 400 °C. The diagrams in this section illustrate the percentage of decrease in strength due to temperature rise. Moreover, the cracks and color of concrete tend to vary due to increased heat, and becomes even more pronounced at temperatures over 400 °C.

Comparing the results of SCC1–SCC4, we observe that the effect of heat on flexural and compressive strength of concrete is related to the maximum concrete compressive strength at 23 °C. In fact, the effect of heat is more pronounced on the concrete with higher compressive strength. A greater reduction was observed in the flexural strength of the specimens with higher compressive strength.

Effect of heat on the moment–curvature diagram

Variations of RCB center under loading indicated that beam friability was proportional to temperature rise. As the concrete was heated, cracks developed due to thermal stresses and temperature difference between the concrete shell and the RCB center. At the longitudinal center of RCB, the cracks led to separation of the concrete from the reinforcing mesh. The effect of temperature variations on the RCB behavior is shown in the moment–curvature diagram (Fig. 4).

As the RCB was exposed to higher temperatures, greater deformations resulted at the concrete beam center during

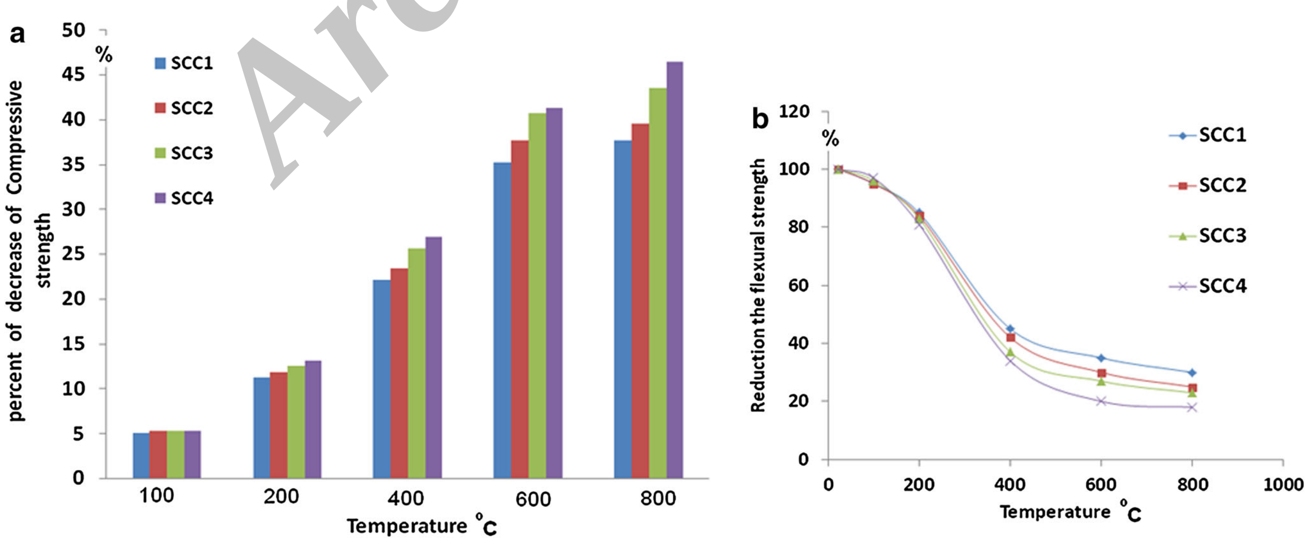

Fig. 3 The diagram shows the percentage reduction of compressive and flexural strengths due to rising temperature

loading, thus lowering the load-bearing capacity of the beam. Initially, only a slight deformation developed in the heated RCB, but it gradually increased as the applied force increased.

The moment–curvature behavior of RCB is linear up to a specific zone, within which the concrete and the internal rebars continuously act against the exerted forces. Such consistency in concrete and steel behaviors dissipates with increased loading. The concrete experiences cracks and the thermal cracks develop into deeper cracks. The moment–curvature diagram entered its non-linear region at lower moments and higher deformations as the RCB absorbed greater heat. Moreover, as the pre-loading temperature in RBC rose, the maximum curvature within the linear (MR) range occurred at greater deformation and lower power. Increased heat led to decreased MY (maximum yield strength of the beam). The curvature of the non-linear range in the heated RCB diagram decreased with increasing heat, leading to increased diagram width.

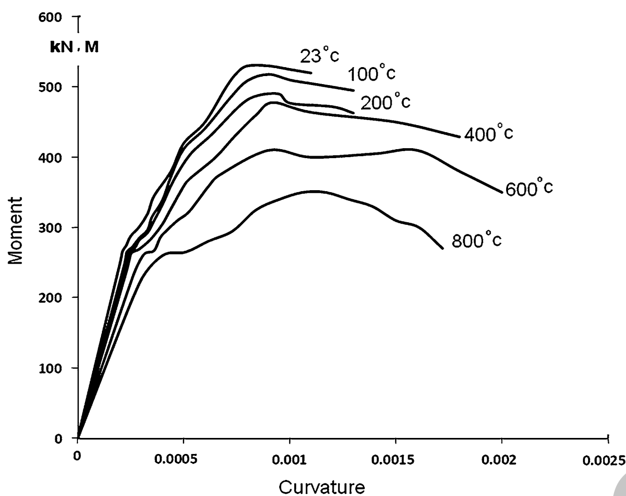

Fig. 4 The moment–curvature diagram in the heated RCBs under uniform axial loading

Effect of heat on the propagation of cracks in concrete

The major cracks in normal or slightly heated RCB specimens were due to loading and appeared at the beam center at an angle with the abutments. However, the RCBs heated to high temperatures showed more concrete friability with cracks further inclined toward a vertical angle. In this state, the concrete was separated from the RCB surface, and the reinforcing mesh was revealed. The concrete heating and cooling was accompanied by cracks developing the concrete surface due to the temperature difference between the concrete center and exterior, which created thermal stresses. At low temperatures, the cracks were tiny and almost invisible. In fact, the cracks at low temperatures were within the shrinkage and creep cracks range (Fig. 5). However, at temperatures close to 400 °C, the concrete specimen, having been exposed to heat for about 40 min of heat, loses its surface vapor and its cracks further deepen. Concrete cracks and separation are also more intense at higher temperatures (Fig. 6).

Fig. 5 The heated RCB under flexural loading at various strengths

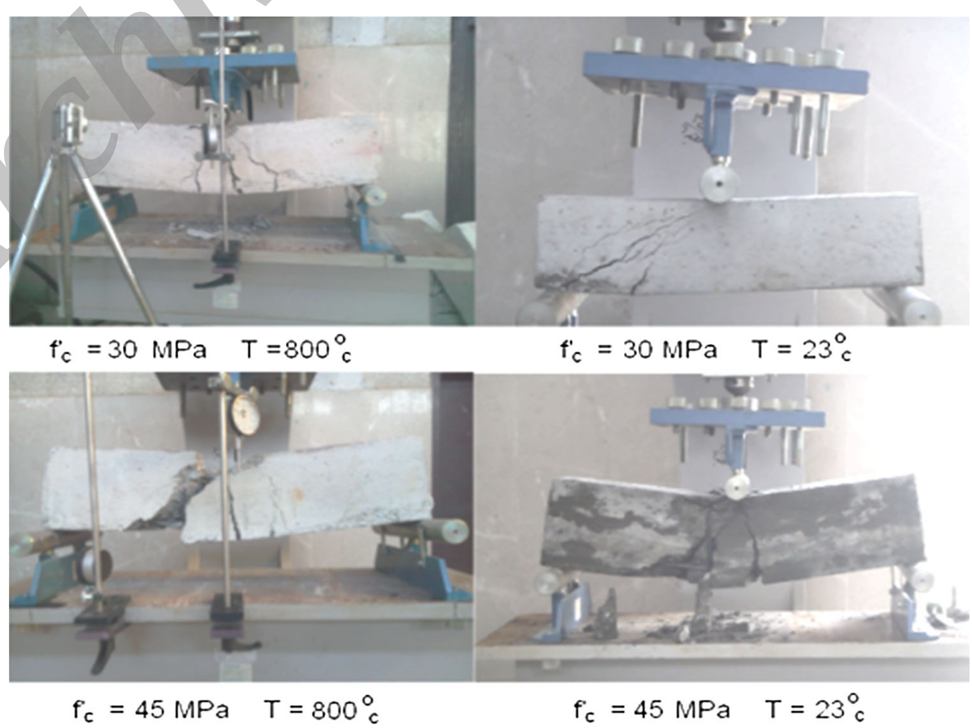

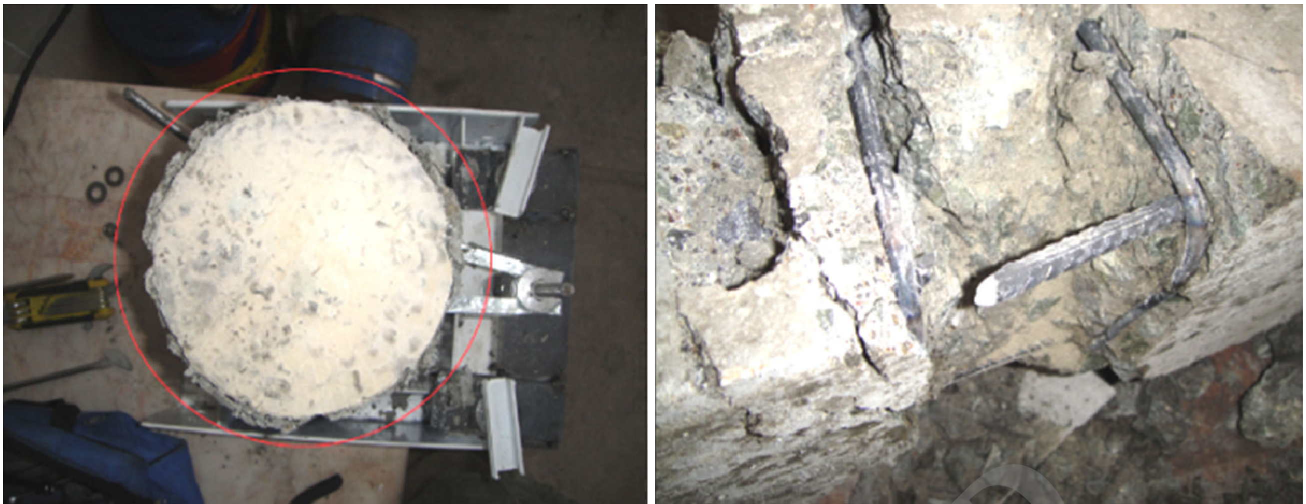

Fig. 6 Crack propagation from the edges of cylindrical concrete samples and its separation from the buried rebars as a result of heating

Table 3 New model

T	$M_t < M_R$	$M_R < M_t < M_y$	$M_y < M_t$	
	$23 < T < 800$	$23 < T < 800$	$23 < T < 400$	$400 < T < 800$
Model	$\frac{M}{13\times10^5}+\frac{0.15\times T}{10^5}$	$\frac{M^2}{13\times10^5\times270}+\frac{T\times M^2}{3\times10^{11}}$	$\frac{M-(575-0.15\times T)}{-5000}$	$\frac{M-(997-0.545\times T)}{-(136{,}365+22.72\times T)}$

T temperature, M moment, M_t moment level, M_y yielding moment

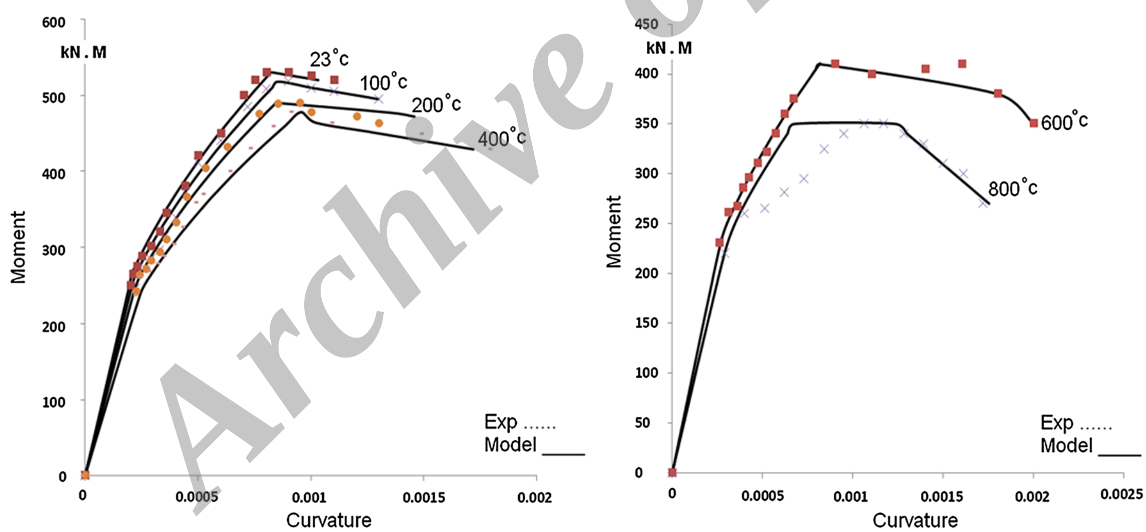

Fig. 7 The moment–curvature diagram proposed for heated RCBs in linear form and the experimental results represented as discrete points

The shape and depth of the cracks depend on the concrete compressive strength and the temperature exerted on the specimen. As the compressive force increases, the cracks begin to spread at the concrete corners. It should be noted that stress concentration is greater at the edges possibly as a result of heat and loading.

The effectiveness of cracks can be determined through measuring the strain at a given stress. This calculation was examined in two ways. In order to calculate the effect of concrete compressive strength, the results of the stress–strain diagram for the heated SCC specimens were compared at a constant temperature for various compressive strengths. The effects of heat-induced cracks and behavioral outcomes were examined through a specific SCC specimen with constant compressive strength under different temperatures. The reduced compressive strengths and increased deformations can be observed in the moment–curvature diagram for RCB and the stress–strain diagram for concrete, respectively. Moreover, there were visible shiny spots on the surface of heated specimens, which were later found to be probably due to the effect of heat on micro silica.

Proposed model for moment–curvature relations

A new model was presented to predict the flexural strength and moment–curvature diagram for heated RCB beams. This model consists of two parts (Table 3). The equation was obtained for the temperature range of 23–800 °C.

Considering that the RCB behavior on the moment–curvature diagram is composed of a linear and a curved part, this model similarly has two parts: the first involves moments lower than the MR level predefined as a constant value within the range 23–800 °C. When the moment on the beam is between MY and MR, the diagram is a curve. Moreover, the diagram behavior varies with the specimen temperature. The variations within the zones before and after 900 °C tend to experience greater difference, requiring modeling too be performed in two parts. The modeled diagram and experimental results are in good agreement and the moment–curvature diagram is modeled in three sections (Fig. 7).

Conclusions

This research aimed to examine the behavior of SCC-heated RCBs with compressive strengths ranging from 30 to 45 MPa. Several standard cylindrical concrete specimens were used to evaluate the effects of different temperatures (23–800 °C). The test results were compared in terms of test parameters, concrete temperature and compressive strength. The results demonstrated that the flexural strength of RCB and the SCC concrete specimens decreased with increasing temperature. The depth and impact of cracking in the heated concrete depended on the compressive strength and temperature of the concrete. The effect of temperature rise was greater for concretes with higher compressive strengths. For more friable concrete specimens, the heat-induced cracks produced a more pronounced reduction in compressive strength. The variations for the specimens mixed at 400 °C increased. This was modeled using the proposed equation.

References

Carreira DJ, Chu KH (1985) Stress–strain relationship for plain concrete in compression. ACI Struct J 82:797–804
Chang YF, Chen YH, Sheu MS, Yao GC (2006) Residual stress–strain relationship for concrete after exposure to high temperatures. Cem Concr Res 36:1999–2005
Cioni P, Croce P, Salvatore W (2001) Assessing fire damage to r.c. elements. Fire Saf J 36:181–199
Dwaikat MB, Kodur VKR (2009) Response of restrained concrete beams under design fire exposure. J Struct Eng 135(11):1408–1417
Huang SS, Burgess IW (2012) Effect of transient strain on strength of concrete and CFT columns in fire—part 1: elevated-temperature analysis on a Shanley-like column model. Eng Struct 44:379–388
Huang Z, Burgess IW, Plank RJ (2009) Three-dimensional analysis of reinforced concrete beam-column structures in fire. J Struct Eng 135(10):1201–1212
Huo J, Zhang J, Wang Z, Xiao Y (2013) Effects of sustained axial load and cooling phase on post-fire behavior of reinforced concrete stub column. Fire Saf J 59:76–87
Khennane A, Baker G (1993) Uniaxial model for concrete under variable temperature and stress. ASCE J Eng Mech 119:1507–1525
Kim YJ, Hmidan A, Choi KK (2012) Residual behavior of shear-repaired concrete beams using CFRP sheets subjected to elevated high temperatures. J Compos Constr 16(3):253–264
Lo TY, Nadeem A, Tang WCP, Yu PC (2009) The effect of high temperature curing on the strength and carbonation of pozzolanic structural lightweight concretes. Constr Build Mater 23:1306–1310
Mydin MAO, Wang YC (2012) Mechanical properties of foamed concrete exposed to high temperatures. Constr Build Mater 26:638–654
Ranzi G, Bradford MA (2007) Analytical solutions for elevated-temperature behavior of composite beams with partial interaction. J Struct Eng 133(6):788–799
Sancak E, Dursun SY, Simsek O (2008) Effects of elevated temperature on compressive strength and weight loss of the light-weight concrete with silica fume and super plasticizer. Cem Concr Compos 30:715–721
Tan KH, Nguyen TT (2013) Structural responses of reinforced concrete columns subjected to uniaxial bending and restraint at elevated temperatures. Fire Saf J 60:1–13
Tan KH, Zhou Y (2011) Performance of FRP-strengthened beams subjected to elevated temperatures. J Compos Constr 15(3):304–311
Terro MJ (1998) Numerical modeling of the behavior of concrete structures in fire. ACI Struct J 95:183–193
Xu YY, Wu B (2009) Fire resistance of reinforced concrete column with L−, T− and +-shaped cross-sections. Fire Saf J 44:869–880
Youssef MA, Moftah M (2006) General stress–strain relationship for concrete at elevated temperatures. J Eng Struct 29:2618–2634